

A Novel Biosorbent *Lagenaria vulgaris* Shell - ZrO₂ for the Removal of Textile Dye From Water

Milica M. Petrović*, Miljana D. Radović, Miloš M. Kostić, Jelena Z. Mitrović, Danijela V. Bojić, Aleksandra R. Zarubica, Aleksandar Lj. Bojić

ABSTRACT: A new biosorbent, abbreviated as LVB-ZrO₂, was synthesized by chemically modifying *Lagenaria vulgaris* shell with ZrO₂. The removal of textile dye RB19 from aqueous solution by LVB-ZrO₂ was studied. Characterization by SEM, FTIR and XRD confirmed the chemical modification of the biomaterial, which showed significant improvement of removal efficiency compared with unmodified *Lagenaria vulgaris* shell. LVB-ZrO₂ point of zero charge is 5.49. The biosorption process is highly pH dependent and the optimal pH is 2.0, at which complete dye removal was attained. The results are the best by a pseudo-second order kinetic model. The optimal adsorbent dosage is 4 mg/dm³. The RB19 biosorption follows the Langmuir isotherm model ($R^2=0.9978$), with the maximum sorption capacity of 75.12 mg/g. LVB-ZrO₂ is a mechanically stable, easy to synthesize, cost-effective, biocompatible and environmentally-friendly biosorbent with the high potential for the removal of RB19 from aqueous solution. *Water Environ. Res.*, **87**, 635 (2015).

KEYWORDS: biomaterial, modification, ZrO₂, removal, dye.

doi:10.2175/106143015X14212658614838

Introduction

Synthetic dyes are colored aromatic compounds with different chromophores and reactive groups. Reactive Blue 19 (RB19) is an anthraquinone reactive dye, important in dyeing of cellulosic fibers (Zollinger, 2003; Shore, 1995). The textile dyeing industry releases colored effluents into the environment, which can be harmful to the receiving water sources. A large portion of synthetic dye that is lost during the dyeing process could remain mainly intact, because they are stable to light, heat, oxidizing agents and aerobic biological degradation. The application of conventional physicochemical wastewater treatments (precipitation, sedimentation, ultrafiltration, flotation, UV irradiation, ozonation and coagulation) is limited due to the poor dye removal or high operational costs, intensive energy requirement and limited adaptability to a wide range of effluents (Akar et al., 2009; Aksu and Isoglu, 2006; Barka et al., 2013; Singanan, 2003).

Biosorption is a promising alternative technology to remove organic pollutants from aqueous solutions using inactive and dead biomasses as the sorbents, with the advantages of low-cost, availability in nature, greater profitability and ease of operation. Biosorbents are inexhaustible, low-cost and non-hazardous materials, which require little processing. Various biosorbents for dye removal have been applied, such as agricultural waste (Akar et al., 2009; Aksu and Isoglu, 2006) and the different parts of various

plants, such as seeds (Alencar, 2012), shell (Cardoso et al., 2011) and cladodes (Barka et al. 2013). Biomaterials, including dead biomass and biopolymers, can be modified by inorganic materials, such as SiO₂, TiO₂, Fe₂O₃ and others, providing the new, unique hybrid or composite materials (Copello et al., 2011; Mahmoodi et al., 2011; Gupta and Nayak, 2012). Certain modifications of biosorbents by metal oxides may improve their sorption efficiency and mechanical and other properties. Investigations by Copello et al. (2011) and Mahmoodi et al. (2011) have demonstrated that some textile, food, biological and chemical dyes could be effectively removed from water using chitosan hydrogel/SiO₂ and chitin hydrogel/SiO₂ hybrid materials and alginate/titania nanoparticles.

Lagenaria vulgaris is a large annual, climbing or trailing herb that can be grown worldwide, up to 1600 m altitude. It doesn't require use of agrochemicals and specific soil preparation for planting. It is mostly composed of cellulose and lignin (Shah et al., 2010). The shell of *Lagenaria vulgaris* was selected as the starting biosorbent material because it possesses a macro porous structure, very high mechanical stability under various biosorption treatment conditions, it does not swell in water, and its cellulosic structure offers the possibility of chemical modification (Stanković et al., 2013). In addition, it is easily available, environmentally friendly, low cost and easy to grow and prepare. *Lagenaria vulgaris* shell has effectively removed metal cations from water (Mitić-Stojanović et al., 2011; Stanković et al., 2013), but its ability to remove the anionic dye is relatively low. In attempt to improve that ability and to obtain an efficient material for the reactive dye removal, it was modified with a small amount of ZrO₂. To the best of our knowledge, neither *Lagenaria vulgaris*, nor ZrO₂ has been used for that purpose. In this paper, a synthesis, characterization and application of a novel *Lagenaria vulgaris*-ZrO₂ biosorbent for the removal of RB19 from aqueous solution was studied.

Materials and Methods

RB19 with 50% purity was purchased from Dystar (Germany). ZrOCl₂·8H₂O, HNO₃ and NaOH (Merck, Germany) were of analytical reagent grade.

Preparation and Characterization of Biosorbent. The experiments were performed using a shell of *Lagenaria vulgaris*, grown in the south of Serbia (near the town of Niš) at 200 m altitude under controlled conditions with irrigation and without fertilization. All plants were planted at the same time in mid-April and harvested in mid-October. *Lagenaria vulgaris* shell was roughly crushed, washed with deionized water, grounded by laboratory mill, then acid treated (0.3 M HNO₃), washed with deionized water, treated with 1M NaOH 60 min, washed with deionized water, dried in the oven at 55 ± 1 °C to constant weight and abbreviated as LVB. 10 g of LVB was dispersed in 100 cm³ of 10 g/dm³ solution of

* Department of Chemistry, Faculty of Science and Mathematics, University of Niš, Višegradska 33, 18 000 Niš, Serbia; email: milicabor84@gmail.com

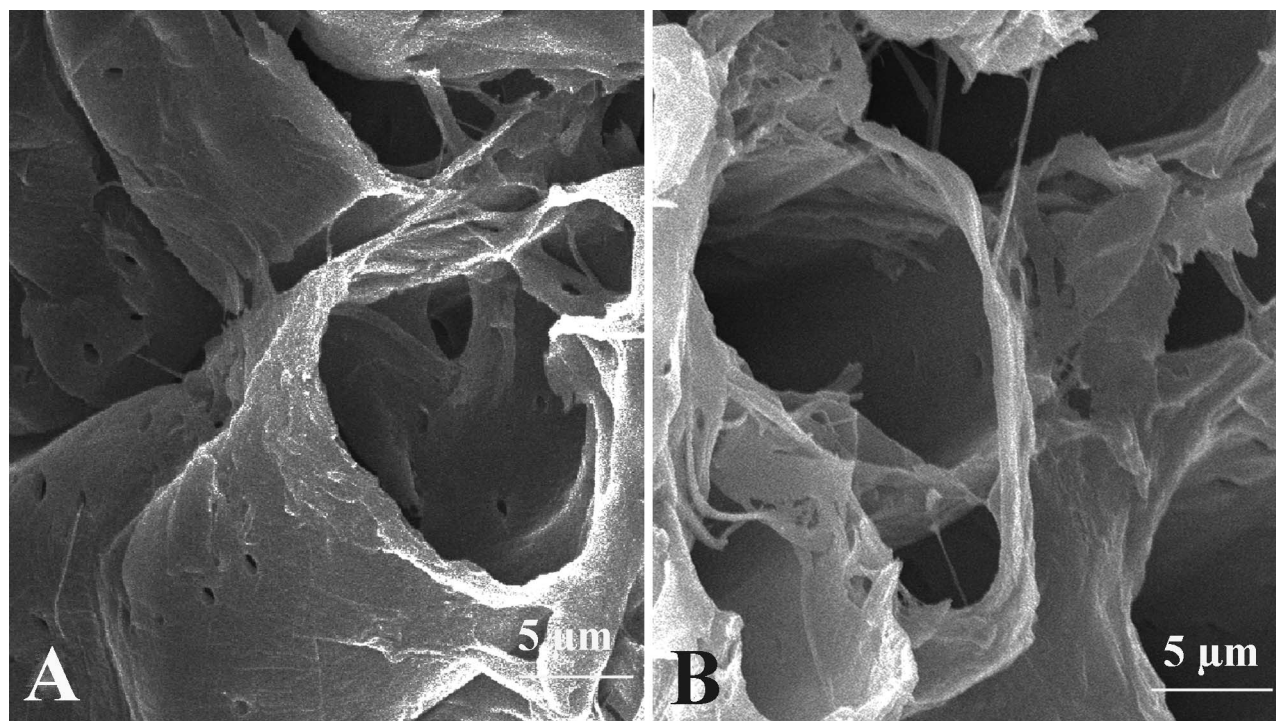


Figure 1—SEM images of: A) LVB and B) LVB-ZrO₂ at magnification of $\times 2000$.

ZrOCl₂·8H₂O. The dispersion was stirred for 0.5 h at 25.0±0.5 °C. After that solution was evaporated. Obtained material was washed with deionized water, treated by trimethylamin, washed with deionized water until neutral pH and dried at 55±1 °C for 5 h. This material was abbreviated as LVB-ZrO₂.

The content of zirconium in the sample was determined using an inductively coupled atomic emission spectrometer model 6500 Duo (Thermo Scientific, United Kingdom) equipped with a CID86 chip detector (the material sample (0.5 g) was digested with a mixture of 7 mL of concentrated HNO₃ and 1 mL of 30 % H₂O₂ in an Advanced Microwave Digestion System (Ethos 1, Milestone, Italy) under the following program: heated up to 200 °C in 10 min and held for 10 min at that temperature). Scanning electron microscopy (SEM) was performed using the lower detector of a Hitachi SU8030 cold-cathode field emission gun scanning electron microscope (FEG-SEM) at 2 kV accelerating voltage, at various working distances between 10 and 16 mm and at nominal magnifications of $\times 200$ and $\times 2000$. XRD pattern was taken by the use of a Siemens D500 diffractometer (Germany) with a Ni filter using Cu K α radiation ($\lambda = 0.154$ nm) and the step-scan mode with a step width of 0.02° and 1 s/step. FTIR spectra were recorded by means of a BOMEM MB-100 FTIR spectrometer (Hartmann & Braun, Canada) using KBr pellets containing 1.0 mg of the sample in 150 mg KBr. The instrument is equipped with a standard DTGS/KBr detector in the range of 4000–400 cm⁻¹ with a resolution of 2 cm⁻¹. Point of zero charge was determined by pH drift method (Yang et al., 2004) with some modifications for LVB-ZrO₂. The pH of test solutions were adjusted in a range between 2 and 10 using 0.01M HNO₃ and 0.01 M KOH. A 0.2 g of biosorbent samples were added to 50 ml of test solutions into stopped glass tubes and equilibrated for 24 h. The final pH (pH_f) was measured after 24 h and plotted against the initial pH (pH_i). The pH at which the curve crosses line pH_i = pH_f was taken as pH_{pzc}.

Batch Sorption Experiments. The stock solutions of RB19 (1.0000 g/dm³) were prepared by dissolving a given amount of powdered RB19 in deionized water. Working model solutions were prepared by the appropriate dilution of the stock solutions. To examine the effect of initial dye concentration, the solutions with 800 and 1600 mg/dm³ of the dye were prepared separately, by directly dissolving the given amount of the powdered dye. The pH of the solutions was adjusted with 0.1/0.01 mol/dm³ NaOH/HNO₃ solutions pH-metrically (SensIon5, HACH, USA). All experiments were performed at 20.0±0.5 °C. The samples of the solution were taken before the adsorption started, and after: 1, 5, 10, 20, 40, 60, 90, 120 and 180 min and analyzed. Dye concentration was measured using UV-vis spectrophotometer Shimadzu UV-1650 PC (Shimadzu, Japan) at 592 nm. The amount of RB19 adsorbed q_t (mg/g) was determined by using the equation:

$$q_t = \frac{(c_0 - c_t)V}{m} \quad (1)$$

where c_0 and c_t are the initial and final dye concentrations (mg/dm³), V is the solution volume (dm³) and m is the mass of the sorbent (g).

The removal efficiency (RE) of RB19 by biosorbent was calculated using the equation:

$$RE(\%) = \frac{c_0 - c_t}{c_0} \times 100 \quad (2)$$

Results and Discussion

Material Characterization. ZrO₂ was almost quantitatively (98.7%) transferred to the biomaterial and its content in LVB-ZrO₂ sorbent was 3.7%. The SEM images of LVB and LVB-ZrO₂ (Figure 1A and 1B) show that the surface structure of the biomaterial before (LVB, Figure 1A) and after incorporation of ZrO₂ (LVB-

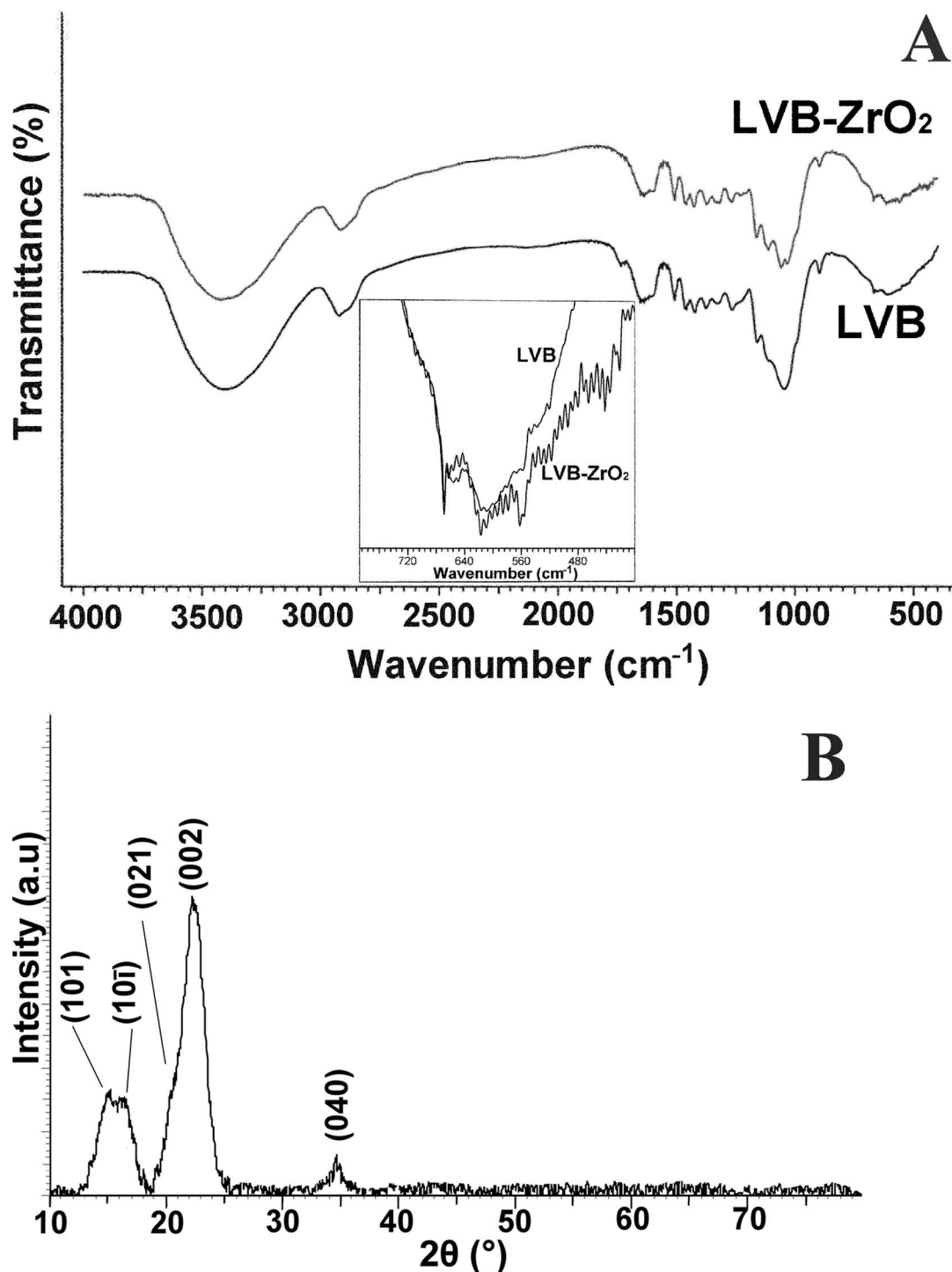


Figure 2—A) FTIR spectra of LVB and LVB-ZrO₂ and B) XRD spectrum of LVB-ZrO₂

ZrO₂, Figure 1B) was very similar, meaning that the process did not bring any visible physical change of the biomaterial surface morphological structure. The surface layers of the LVB-ZrO₂ are smooth, like those of LVB and the visible ZrO₂ layers, particles and/or “islands” as the separate phase on the biomaterial surface were not detected, indicating that ZrO₂ was highly and homogeneously dispersed, without change of the biomaterial structure.

The spectra of LVB and LVB-ZrO₂ are similar (Figure 2A), exhibiting characteristic absorption bands for the lignocellulose

material; a detailed discussion of LVB spectrum is given elsewhere (Stanković et al., 2013; Mitić-Stojanović et al., 2011). In the spectrum of LVB-ZrO₂, the series of small absorption bands below 550 cm⁻¹ corresponding to Zr–O vibrations were detected (Sahu and Rao, 2000; Sarkar et al., 2007), confirming the presence of ZrO₂ in LVB-ZrO₂. Their intensity is somewhat lower due to a relatively low content of ZrO₂ in LVB-ZrO₂.

The XRD pattern of LVB-ZrO₂ shows the peaks that are typical for cellulosic materials with relatively high portions of

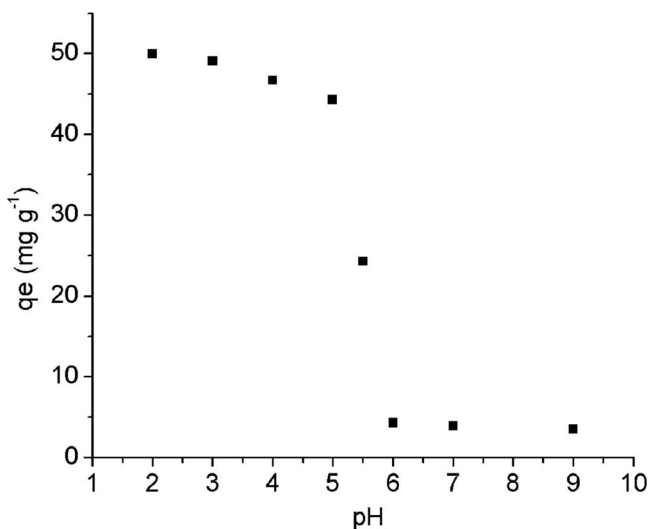


Figure 3—Effect of initial pH on the removal efficiency for RB19 from 50.0 mg/dm³ solutions by 4.0 g/dm³ LVB-ZrO₂ biosorbent at 20 ± 0.5 °C at equilibrium.

crystalline regions (Figure 2B). The series of broad, well defined peaks with 2 theta values at: 15.0°, 16.6°, 20.7°, 22.7° and 34.5° correspond to (101), (10i), (021), (002) and (040) reflection, respectively (Park et al., 2010). The XRD pattern of LVB-ZrO₂ does not contain characteristic peaks that appear in the XRD pattern of any crystalline modification of ZrO₂ (Noh et al., 2003), meaning that it doesn't exhibit its individual characteristics, though its presence in the material was confirmed.

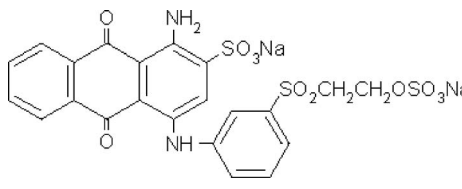
The absence of ZrO₂ peaks in the XRD pattern of LVB-ZrO₂ is in accordance with the result obtained by SEM analysis, which did not detect ZrO₂ as a separate phase on the biomaterial surface. It can be assumed that LVB-ZrO₂ is a unique, highly crystalline cellulosic material, where ZrO₂ is bound to a biomass in such a way that it does not exhibit its individual XDR characteristics. This fact, as well as its absorption bands presented in the FTIR spectrum of LVB-ZrO₂, indicates that it is probably chemically bonded to the biomaterial functional groups in a certain way.

The point of zero charge (pH_{pzc}) of LVB-ZrO₂ is 5.49, meaning that at pH lower than 5.49, its surface is positively charged and at pH higher than 5.49, it is negatively charged. The pH_{pzc} of LVB is 6.10, meaning that the modification made the material a little more acidic.

Batch Biosorption Experiments. *Effect of pH.* LVB generally possesses good cation removal efficiency (Mitić-Stojanović et al., 2011), but its ability to adsorb the anions is poor; only 24.5% of RB19 was removed from 50 mg/dm³ solution by LVB at equilibrium at optimal pH (results not shown). However, its chemical modification with ZrO₂ resulted in the material with a high efficiency of anionic dye RB19 removal. The pH significantly affects the removal process (Figure 3).

At lower, acidic pH, the RB19 removal is much higher than at neutral and alkaline pH. At pH 2 complete dye removal at equilibrium is attained, and it decreases slightly as the pH increases up to 5, though it still remains relatively high (98.21, 93.40 and 90.02% at pH 3, 4 and 5, respectively). At pH higher than 5, the dye removal rapidly decreases and it falls below 9% at

Table 1—Main characteristics of Reactive Blue 19.

Characteristic	Reactive Blue 19
Chemical structure	
C.I. generic name	Reactive Blue 19
Synonym	Remazol Brilliant Blue R
IUPAC name	
Molar mass (g mol⁻¹)	626.50
λ_{max} (nm)	592

pH 6. Further increase in pH practically does not affect the adsorption. RB 19 has sulfonic groups (Table 1), which are negatively charged even in highly acidic solutions (Zollinger, 2003). The biosorbent surface net charge is pH-dependent. At pH values up to 5, it was protonated and positively charged. Thus, RB19 was bound to a biosorbent surface via electrostatic interactions. With the increasing medium pH, the net positive charge of the surface decreases and the dye uptake decreases as well. A sudden decrease of the dye uptake is observed between pH 5 and 6. At pH 5.5, which is very close to the material pH_{pzc}, it is approximately half of the maximal q_e value, obtained at pH 2. At pH higher than pH_{pzc} the sorbent surface becomes negatively charged, the dye binding rapidly decreases, reaching its minimum at pH 6, and remaining constant with further increases in pH. The effect of pH on the sorption of RB19 on LVB-ZrO₂ is similar to that reported in the literature for the adsorption of reactive dyes by various biosorbents (Alencar, 2012; Akar et al., 2009; Aksu and Isoglu, 2006; Barka et al., 2013) and by metal oxide modified biomaterials (Copello et al., 2011; Mahmoodi et al., 2011). For most of those biosorbents, the dye sorption rapidly decreases when the pH is higher than 3 to 4. However, in the case of RB19 sorption by LVB-ZrO₂, high dye uptake at equilibrium is attained even at pH 5. That result is somewhat similar to those obtained for the sorption of reactive dyes by inorganic oxide modified materials (Copello et al., 2011; Mahmoodi et al., 2011).

It can be assumed that the main binding mechanism is electrostatic attraction between negatively charged dye molecules and positively charged sorbent surface. At pH 6 and higher, the material has adsorbed a certain amount of RB19 as well, indicating that electrostatic attraction is not the only sorption mechanism. Some other kind of attraction, like polar attraction between adsorbent and adsorbate, may play a certain role in the whole process and that attraction is the sorption driving force at pH higher than 6. However, electrostatic attraction is the dominant adsorption mechanism at pH lower than 5, where complete (pH 2) or almost complete (pH 3 to 5) dye removal was attained.

Effect of Adsorbent Dosage. At lower adsorbent dosages, increasing biosorbent dosage resulted in a sharp increase in the biosorption yield (Figure 4A). The increase in adsorbent dosage from 0.5 to 1.0 g/dm³ resulted in an increase of RB19 removal

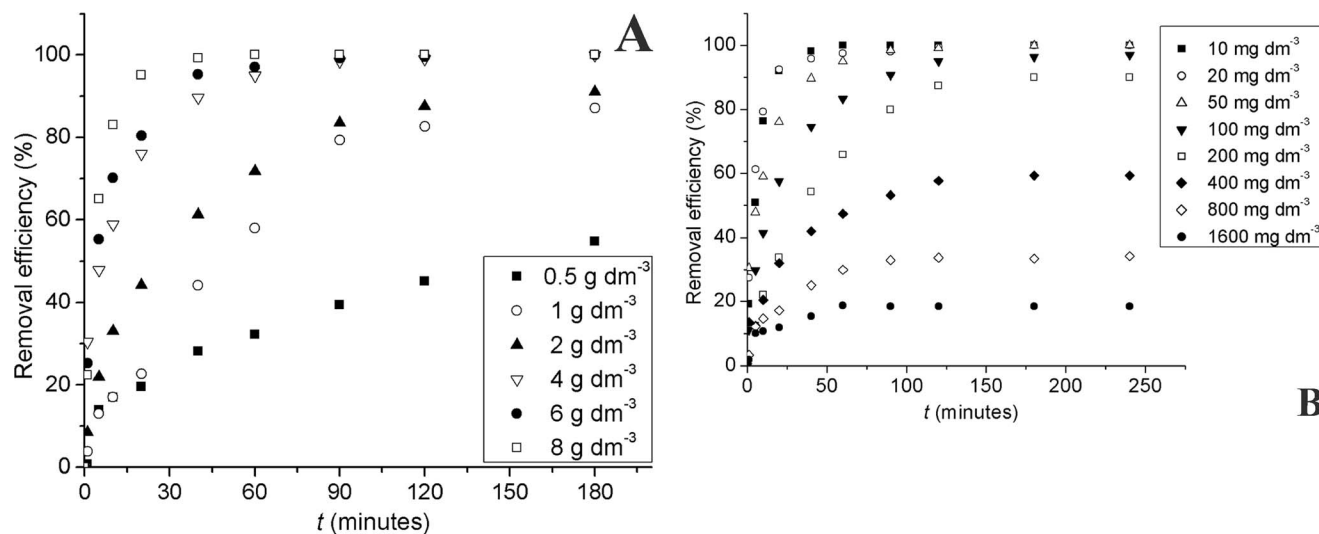


Figure 4—Effect of A) LVB-ZrO₂ dosage on the removal of 50.0 mg/dm³ RB19 and B) initial RB19 concentration on its removal by 4.0 g/dm³ LVB-ZrO₂ (20±0.5 °C, pH 2.0).

efficiency from 54.7 to 87.2%, and increase in dosage from 1.0 to 2.0 g/dm³ increased removal efficiency from 87.2 to 91.1%, and that from 2.0 to 4.0 g/dm³ from 91.1 to 99.5%. A further increase of the adsorbent dosage to 6.0 g/dm³ and to 8.0 g/dm³ did not have a significant effect on dye removal, which increased by only 0.3% for both of the concentrations, so the optimal biosorbent dosage for this process is 4.0 g/dm³.

A rapid increase in dye removal efficiency with the increasing adsorbent dosage occurred due to an increase in the surface area of the biosorbent and in the number of possible binding sites for RB19. A further increase in biosorbent concentration over 4.0 g/dm³ did not result in a significant increase in biosorption yield, which probably occurred due to an overlapping or partial aggregation of the biosorbent particles, resulting in a decrease in effective surface area for the dye sorption. A similar effect was

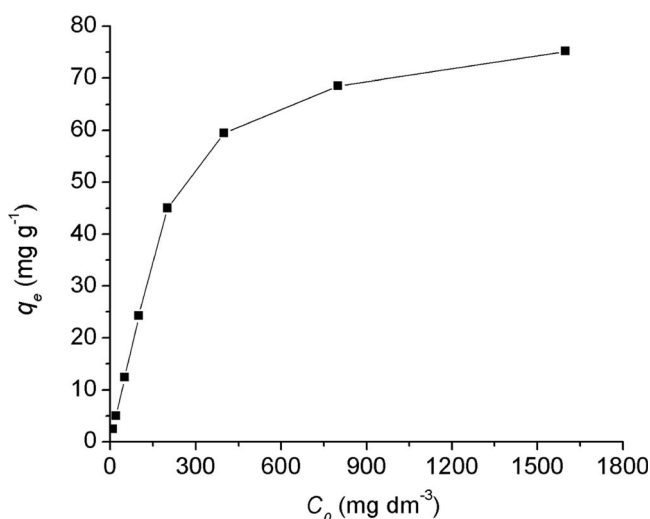


Figure 5—Effect of the initial concentration on the adsorbed amount of RB19 onto LVB-ZrO₂ at equilibrium (LVB-ZrO₂ dosage 4.0 g/dm³, 20±0.5 °C, pH 2.0)

reported by other authors (Akar et al., 2009; Barka et al., 2013; Davila-Jimenez et al., 2009).

Effect of Initial Dye Concentration. For the initial RB19 concentration of 10 and 20 mg/dm³, the removal efficiency reached 100%, and for the 50 mg/dm³ it reached 99.7% (Figure 4B). For initial concentrations of 100 and 200 mg/dm³, removal efficiency was still over 90%, but it sharply decreased to 59.3% for the initial dye concentration of 400 mg/dm³, and to 18.6% for 1600 mg/dm³ of the dye.

In the case of lower concentrations, the ratio of initial number of dye anions to the available sorption sites is low and the biosorption becomes independent of initial concentration, which enabled the 100% dye uptake. At higher concentrations, a certain amount of dye ions are left unadsorbed in the solution due to a saturation of the limited available binding sites in the biomass and the removal of dye depends on the initial concentration (Aksu and Isoglu, 2006). However, comparing q_e values for different initial dye concentrations, a gradual increase in binding with increasing initial dye concentration is observed. The q_e sharply increases for the initial dye concentrations up to 200 mg/dm³ and it does not significantly change from 800 to 1600 mg/dm³, the highest initial dye concentration tested, at which it reaches an adsorption capacity of 75.12 mg RB19 per g of LVB-ZrO₂ (Figure 5). This implies that the absolute adsorbed amount of RB19 onto the biomass is enhanced upon increasing the initial concentration, i.e. higher initial concentration of RB19 will enhance the adsorption process.

Sorption Kinetics. The kinetics of RB19 adsorption on LVB-ZrO₂ can be described by the pseudo-second order model and intraparticle diffusion kinetic model.

The pseudo-second-order equation (Ho and McKay, 1998) based on equilibrium adsorption can be expressed as follows:

$$\frac{1}{q_t} = \frac{1}{k_2 q_e^2} + \frac{1}{q_e} t \quad (4)$$

where k_2 is the pseudo-second-order reaction rate constant (g/mg·min).

The experimental data fit well to the pseudo-second order equation (Figure 6). The corresponding R^2 values are close to unity (Table 2).

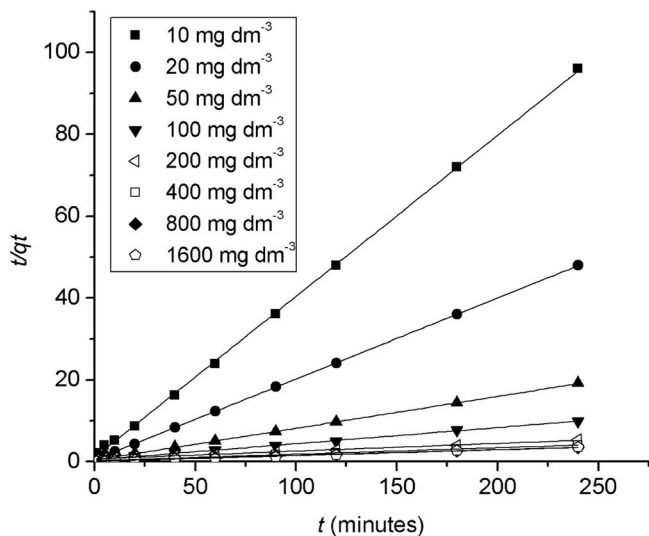


Figure 6—Pseudo-second-order kinetics for adsorption of RB19 on 4.0 g/dm³ LVB-ZrO₂ at 20 ± 0.5 °C and pH 2.0.

The calculated q_e values for RB19 were relatively close to the experimental q_e values suggesting that dye sorption by LVB-ZrO₂ approximately follows a pseudo-second-order reaction. The good fit to the pseudo-second-order kinetics indicates that the adsorption mechanism depends on the nature of adsorbate and adsorbent; the rate-limiting step is probably a chemical process and the sorption mechanism is based on ion exchange between positively charged surface of biosorbent and negatively charged dye molecules. The corresponding rate constants decrease with an increase in initial dye concentration, which is attributed to the lower competition for the sorption surface sites at lower concentrations; at higher concentrations, the competition for the surface active sites is high, thus the corresponding sorption rates are lower (Chen et al., 2010).

The possibility of intra-particle diffusion was explored by using the intra-particle diffusion kinetics model (Weber Jr. and Morris, 1964), which can be represented by the equation:

$$q_t = K_{id}t^{1/2} + C \quad (6)$$

where C is the intercept, and K_{id} is the intraparticle diffusion constant (mg/g•min^{1/2}) determined from a plot q_t versus $t^{1/2}$.

Relatively high corresponding R^2 values (Table 2) obtained from experimental data for this model, imply that the intra-particle diffusion had been significant. The two linear sections with different slopes (Figure 7) indicate that the adsorption process exhibits two stages: the first linear part is attributed to intraparticle diffusion through macropores and the second stage to diffusion through micropores, followed by the establishment of equilibrium. It was revealed by the SEM (Figures 1A and 1B) that LVB and LVB-ZrO₂ biosorbent have the large pores and channels of more than 10 μm in their structure, and smaller pores of about 1 μm or less are also seen in places. A good agreement with the intraparticle diffusion kinetics model indicates that the diffusion through micropores plays an important role in the sorption process as well.

R^2 values obtained for the two applied kinetics models indicate that the intraparticle diffusion is not the only rate-limiting step, but also other kinetic models may control the rate of adsorption, all of which may be operating simultaneously. The higher R^2 values obtained for the pseudo-second-order model indicate that the chemical process, i.e. ion exchange is the predominant rate controlling process for the adsorption of RB19 on LVB-ZrO₂.

Adsorption Isotherm. The adsorption of RB19 onto LVB-ZrO₂ biosorbent follows the Langmuir isotherm model (Langmuir 1918). The Langmuir parameters are determined from a linearized form of the Langmuir equation:

$$\frac{C_e}{q_e} = \frac{1}{K_L q_{max}} + \frac{1}{q_{max}} C_e \quad (7)$$

where C_e is the equilibrium dye concentration in the solution (mg/dm³), q_e is the amount of dye adsorbed onto the unit adsorbent mass (mg/g), q_{max} is the Langmuir equilibrium constant related to maximum adsorption capacity and K_L is the Langmuir constant which is related to the adsorption enthalpy (dm³/mg). The Langmuir isotherm model makes it possible to predict if an adsorption system is favorable or unfavorable by calculating R_L , a dimensionless constant referred to as the equilibrium parameter using the following equation:

$$R_L = \frac{1}{1 + K_L C_0} \quad (8)$$

The fitting of the data to the Langmuir isotherm (Figure 8) shows that the biosorption of RB19 onto LVB-ZrO₂ follows the Langmuir model. This implies that the uptake of RB19 anions

Table 2—A comparison of pseudo-second order and intraparticle diffusion kinetic models rate constants and calculated equilibrium from experimental data. (Definitions of the parameters listed are given in the main text).

Parameter	Concentration of initial RB 19 solution (mg/dm ³)							
	10	20	50	100	200	400	800	1600
q_e^{exp}	2.475	4.975	12.45	24.2501	44.9950	59.4751	68.5002	75.1200
Pseudo-second order								
k_2 (g/mg•min)	0.1451	0.0773	0.0152	0.0032	0.0012	0.0011	0.0010	0.0010
q_e^{cal}	2.5081	5.0620	12.8172	25.3678	48.2481	63.0915	72.7272	70.4225
R^2	0.9997	0.9999	0.9997	0.9987	0.9964	0.9956	0.9969	0.9932
Intraparticle diffusion model								
k_{i1}	0.5554	1.0620	1.7021	2.7993	4.322	5.0042	7.0487	7.4848
C_1	0.0006	0.2977	1.4840	0.7274	1.858	7.0098	3.5578	9.4066
R^2	0.9864	0.9520	0.9347	0.98034	0.9917	0.9627	0.972627	0.8846

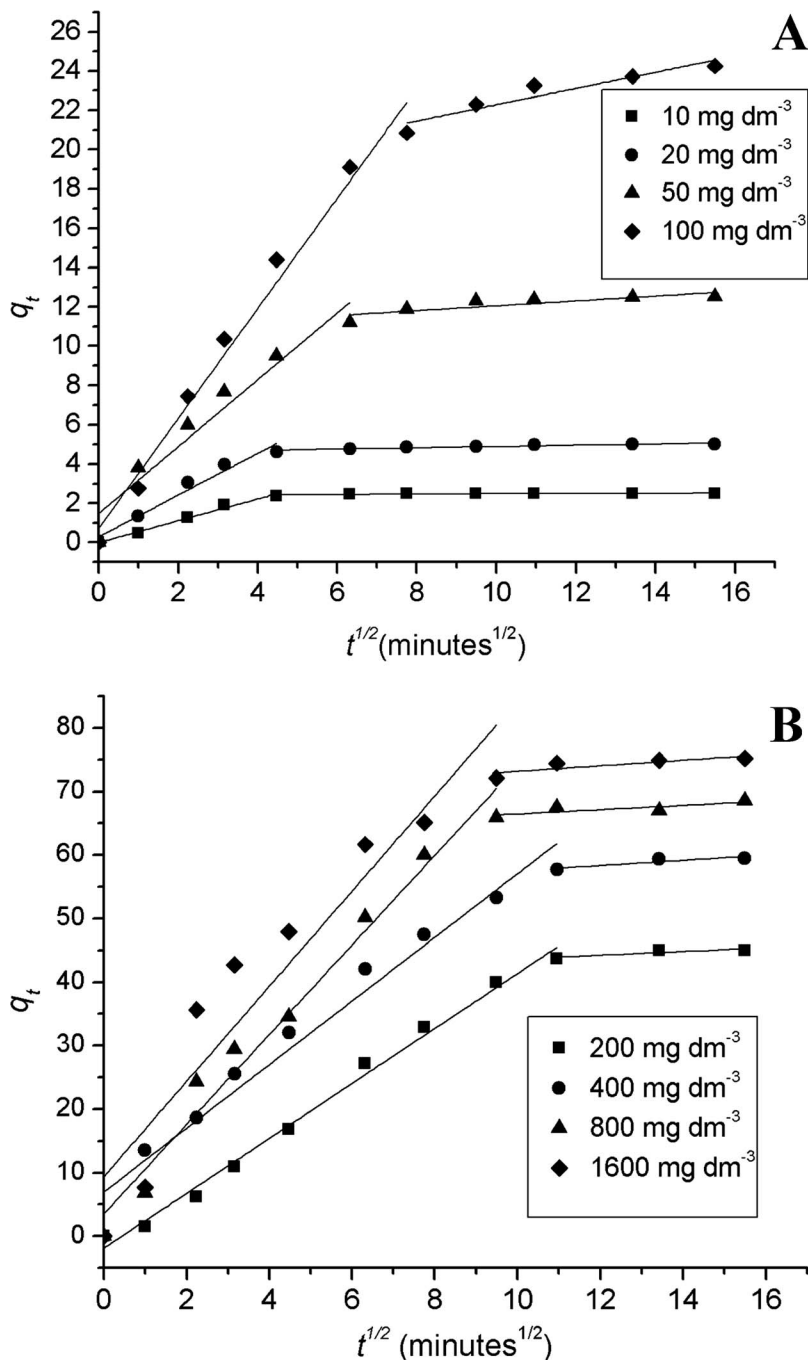


Figure 7—Intraparticle diffusion plot for the adsorption of RB19 on LVB-ZrO₂ for initial dye concentration: A) 10.0–100.0 mg/dm³ and B) 200.0–1600.0 mg/dm³ (4.0 g/dm³ LVB-ZrO₂, 20±0.5 °C, pH 2.0).

occurs on a homogeneous surface by monolayer adsorption without interaction between adsorbed anions, which further implies that all the adsorption active sites are energetically equivalent and the surface is uniform. The equilibrium is established when a monolayer is formed at the adsorbent. The absence of interactions between adsorbed anions indicates that the chemical mechanism of sorption prevails and it is probably ion exchange, which is in accordance with the results obtained from the kinetics studies, as well as with those obtained by the study of the pH effect on the examined adsorption process. The

Langmuir constant (R_L) values are between 0.3871 (for the lowest initial dye concentration) and 0.0039 (for the highest initial dye concentration), meaning that the adsorption process is favorable and the calculated q_{max} value is 74.8503 mg/g (Table 3), which is close to the experimentally obtained q_{max} value (75.12 mg/g).

Conclusion

The new material, LVB-ZrO₂ was synthesized by chemically modifying *Lagenaria vulgaris* shell biosorbent with ZrO₂ in

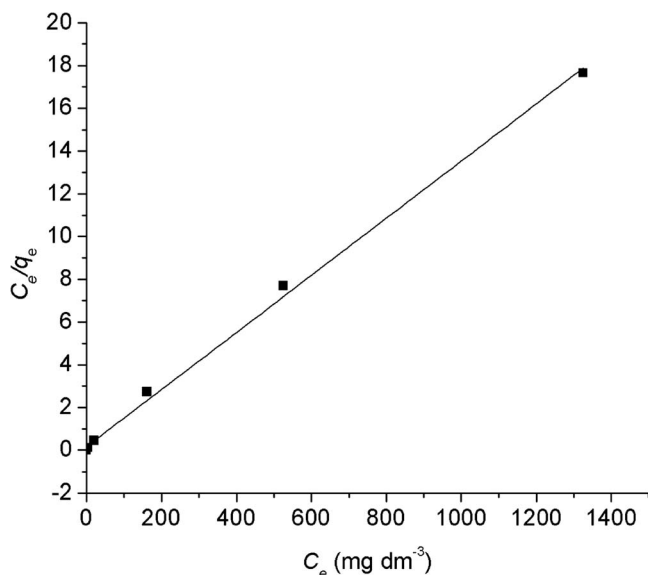


Figure 8—Langmuir isotherm model plot for the adsorption of RB19 on LVB-ZrO₂ (initial dye concentration 10.0–1600 mg/dm³, 4.0 g/dm³ at 20±0.5 °C, pH 2.0).

order to improve RB19 removal ability of untreated biomaterial from aqueous medium. Modification of the biosorbent was confirmed by FTIR spectrum analysis. The content of ZrO₂ in LVB-ZrO₂ sorbent is 3.7%. SEM micrographs showed that the chemical modification did not change the biomaterial morphological structure. No separate ZrO₂ phase was detected in LVB-ZrO₂ XRD pattern, further indicating the chemical bond between ZrO₂ and the biomaterial functional groups. LVB-ZrO₂ showed significant sorption improvement compared with LVB. The adsorption system follows pseudo-second-order kinetics, indicating that chemisorption is the rate-limiting step that controls the adsorption. The adsorption process can also be well described by the two-stage intra-particle diffusion model, indicating that both a chemical and diffusion processes are involved in the biosorption of RB19 onto LVB-ZrO₂. The initial pH strongly affects the sorption of RB19 onto LVB-ZrO₂. Its point of zero charge is 5.49. Complete dye removal is attained at pH 2, which is an optimal pH for the process; as the pH increases up to 5, dye removal slightly decreases, but it still remains over 90% at pH 5; at pH higher than 5, dye removal rapidly decreases, reaching its minimum at pH 6, and remaining constant at pH higher than 6, indicating that the adsorption mechanism is ionic exchange between positively charged sorbent surface and negatively charged dye ions. The extent RB19 removal is directly related to the concentration of LVB-ZrO₂ in the suspension, with an optimal biosorbent dose of 4.0 g/dm³. The Langmuir isotherm model showed the best fit to experimental data in describing the adsorption of RB19 on biosorbent. The maximum adsorption capacity is 75.12 mg RB19 per g of LVB-ZrO₂. In addition to the high removal efficiency, LVB-ZrO₂ possesses other benefits, like mechanical stability, ease of synthesis, cost-effectiveness, biocompatibility and environmental-friendliness, which all makes it a promising material for the removal of anionic pollutants from wastewaters.

Table 3—Langmuir parameters for the adsorption isotherm of RB19 by LVB-ZrO₂ biosorbent.

Constant	Value
q_{max} (mg g ⁻¹)	74.8503
K_L (dm ⁻³ mg ⁻¹)	0.1583
R^2	0.9978

Acknowledgements

This work was supported by the Ministry of Education, Science and Technological development of the Republic of Serbia, Grant No. TR34008.

Submitted for publication ; accepted for publication .

References

- Akar, S. T.; Özcan, A. S.; Akar, T.; Özcan, A.; Kaynak, Z. (2009) Biosorption of a Reactive Textile Dye from Aqueous Solutions Utilizing an Agro-Waste. *Desalination*, **249**, 757–761.
- Aksu, Z.; Isoglu, I. A. (2006) Use of Agricultural Waste Sugar Beet Pulp for the Removal of Gemazol Turquoise Blue-G Reactive Dye from Aqueous Solution. *J. Hazard. Mater. B*, **137**, 418–430.
- Alencar, W. S.; Acayanka, E.; Lima, E. C.; Royer, B.; de Souza, F. E.; Lameira, J.; Alves, C. N. (2012) Application of Mangifera Indica (Mango) Seeds as a Biosorbent for Removal of Victazol Orange 3R Dye from Aqueous Solution and Study of the Biosorption Mechanism. *Chem. Eng. J.*, **209**, 577–588.
- Barka, N.; Ouzaouit, K.; Abdennouri, M.; Makhfouk, M. E. (2013) Dried Prickly Pear Cactus (Opuntia Ficus Indica) Cladodes as a Low-Cost and Eco-Friendly Biosorbent for Dyes Removal from Aqueous Solutions. *J. Taiwan Inst. Chem. Eng.*, **44**, 52–60.
- Cardoso, N. F.; Lima, E. C.; Pinto, I. S.; Amavisca, C. V.; Royer, B.; Pinto, R. B.; Alencar, W. S.; Pereira, S. F. P. (2011) Application of Cupuassu Shell as Biosorbent for the Removal of Textile Dyes from Aqueous Solution. *J. Environ. Manage.*, **92**, 1237–1247.
- Chen, H.; Gai, D.; Zhao, Y.; Zhong, A.; Wu, J.; Yan, H. (2010) Removal of Copper (II) Ions by a Biosorbent—Cinnamomum Camphora Leaves Powder. *J. Hazard. Mater.*, **177**, 228–236.
- Copello, G. J.; Mebert, A. M.; Raineri, M.; Pesenti, M.; Diaz, L. E. (2011) Removal of Dyes from Water Using Chitosan Hydrogel/SiO₂ and Chitin Hydrogel/SiO₂ Hybrid Materials Obtained by the Sol–Gel Method. *J. Hazard. Mater.*, **186**, 932–939.
- Gupta, V. K.; Nayak, A. (2012) Cadmium Removal and Recovery from Aqueous Solutions by Novel Adsorbents Prepared from Orange Peel and Fe₂O₃ Nanoparticles. *Chem. Eng. J.*, **180**, 81–90.
- Ho, Y. S.; McKay, G. (1998) Kinetic Models for the Sorption of Dye from Aqueous Solution by Wood. *Process. Saf. Environ.*, **76**, 183–191.
- Langmuir, I. (1918) The adsorption of gases on plane surfaces of glass, mica and platinum. *J. Am. Chem. Soc.*, **40**, 1361–1403.
- Mahmoodi, N. M.; Hayati, B.; Arami, M.; Bahrami, H. (2011) Preparation, Characterization and Dye Adsorption Properties of Biocompatible Composite (Alginate/Titanium Nanoparticle). *Desalination*, **275**, 93–101.
- Mitić-Stojanović, D. L.; Zarubica, A.; Purenović, M.; Bojić, D.; Anđelković, T.; Bojić, A. (2011) Biosorptive Removal of Pb²⁺, Cd²⁺ and Zn²⁺ Ions from Water by *Lagenaria vulgaris* Shell. *Water SA*, **37**, 1–10.
- Noh, H.; Seo, D.; Kim, H.; Lee, J. (2003) Synthesis and Crystallization of Anisotropic Shaped ZrO₂ Nanocrystalline Powders by Hydrothermal Process. *Mater. Lett.*, **57**, 2425–2431.
- Park, S.; Baker, J. O.; Himmel, M. E.; Parilla, P. A.; Johnson, D. K. (2010) Cellulose Crystallinity Index: Measurement Techniques and their Impact on Interpreting Cellulase Performance. *Biotechnol. Biofuels.*, **3**, 1–10.

- Sahu, H. R.; Rao, G. R. (2000) Characterization of Combustion Synthesized Zirconia Powder by UV-vis, IR and Other Techniques. *Bull. Mater. Sci.*, **23**, 349–354.
- Sarkar, D.; Mohapatra, D.; Ray, S.; Bhattacharya, S.; Adak, S.; Mitra, N. (2007) Synthesis and Characterization of Sol–Gel Derived ZrO₂ Doped Al₂O₃ Nanopowder. *Ceram. Int.*, **33**, 1275–1282.
- Shah, B. N.; Seth, A. K.; Desai, R. V. (2010) Phytopharmacological Profile of Lagenaria Siceraria: A Review. *Asian J. Plant Sci.*, **9**, 152–157.
- Shore, J. (1995) *Cellulosic Dyeing*. Society of Dyers and Colourists: Bradford, UK.
- Singanani, M. (2003) Studies On The Color Removal of Industrial Wastewater By Using Biomaterials-A New Method. In *Water and Environment: Wastewater treatment and Waste Management*; Singh, V. P., Yadavo, R. N., Eds; Allied Publishers: New Delhi, India.
- Stanković, M. N.; Krstić, N. S.; Slipper, I. J.; Mitrović, J. Z.; Radović, M. D.; Bojić, D. V.; Bojić, A. Lj. (2013) Chemically Modified Lagenaria Vulgaris as a Biosorbent for the Removal of Cu^{II} from Water. *Aust. J. Chem.*, **66**, 227–236.
- Weber, W. J. Jr; Morris, J. C. (1964) Kinetics of Adsorption on Carbon from Solution. *J. Sanit. Eng. Div., Am. Soc. Civ. Eng.*, **89**, 31–59.
- Yang, Y.; Chun, Y.; Sheng, G.; Huang, M. (2004) pH Dependence of Pesticide Adsorption by Wheat-Residue Derived Black Carbon. *Langmuir*, **20**, 6736–6741.
- Zollinger, H. (2003) *Color Chemistry, third edition*; VHCA: Zürich, Switzerland.